ACS OMEGA

http://pubs.acs.org/journal/acsodf

Article

Failure Mechanism of Gas-Bearing Coal during Outburst and a New Method for Outburst Prediction

Chengwu Li, Heng Zhang,* Min Hao,* and Xiaoqi Sun

Cite This: *ACS Omega* 2021, 6, 31253−31259

Read Online

ACCESS | Metrics & More | Article Recommendations

ABSTRACT: Coal and gas outbursts are among the most serious disasters affecting the safety of coal mines. Gas is an important factor in these types of disasters. To analyze the characteristics of the damage caused by gas to the coal body during the sudden release of the gas process, a self-developed high-pressure gas release cause coal particle ejection experiment device was used to conduct gas release experiments under different conditions. The results show that at the moment of gas release, coal particles and gas are ejected at high speed, crushing coal particles into smaller particles. With the increase in gas pressure and gas adsorption performance, the crushing effect will increase. Also, the coal ejection strength (CES) will increase nonlinearly. By analyzing the mass ratio of ejected coal particles, based on the theory of crushing work and energy, we developed a new coal particle fragmentation index, which can be fitted linearly to CES. The index is based on the *f* value, which makes up for the limitations of the forecasting method, and can be used more flexibly to predict the coal sample crushing situation. Moreover, the fitting parameter values can more accurately describe the coal particle crushing grade.

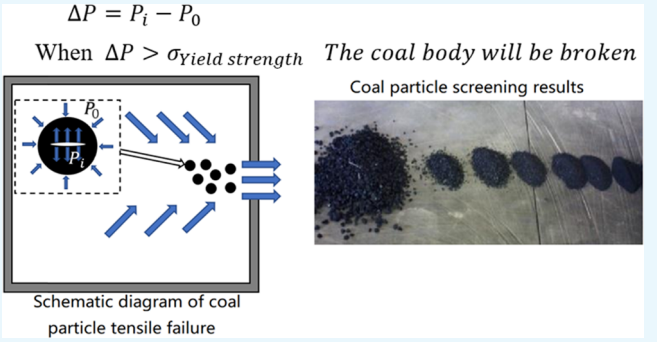

1. INTRODUCTION

The geological conditions of underground coal mine gradually become more complicated with the increase of mining depth, and in situ stress and gas pressure also gradually increase, leading to increasingly serious mine dynamic disasters such as rock bursts and coal and gas outbursts.[1,2] China accounted for about 50% of all outburst events.[3,4] When coal and gas outburst occurs, an enormous amount of coal and gas are ejected from the coal seam, and coal is quickly broken and moved to the coal mining work face. The entire process consumes an extensive amount of outburst energy and produces crushed coal and pulverized coal. Therefore, studying the coal crushing characteristics during the ejection process plays an important role in understanding the coal and gas outburst mechanism.

Owing to the complex conditions in coal mines, it is difficult to study the occurrence process and mechanism of dynamic disasters on site. Therefore, laboratory testing has become a common and effective research method. The experimental research on coal and gas outburst has never stopped. Previous researchers have developed some experimental equipment for outburst simulation. Zhou et al. used a large-scale test system to study outburst experiments under different gas pressures and analyzed the influence of gas pressure on coal migration and outburst strength.[5] Wang et al. found that the effect of gas pressure on outburst is hundreds of times that of in situ stress through experiments.[6] Dai et al. found that the outburst primary energy sources are the internal energy of gas and the elastic potential energy of coal. The energy loss is used to promote coal crushing and ejection.[7] Yin et al. improved the previous outburst experimental equipment and designed a new large-scale outburst simulation equipment to make up for the shortcomings of the previous equipment.[8]

As shown in the above research results, outburst is a fairly complicated process, and the occurrence of outburst is determined by a combination of many factors, such as gas pressure, in situ stress, and geological conditions. After long-term research, the theory that can systematically explain the outburst mechanism is not perfect.[9,10] Therefore, it is impossible to accurately predict coal and gas outbursts. The essence of the outburst is the crushing of the coal body and the ejection of gas. The higher the energy of the coal seam, the greater the risk of outburst and the more seriously the coal body is broken. Therefore, coal fragmentation can reflect the outburst hazard level to a certain extent. Previous researchers

Received: September 10, 2021
Accepted: October 27, 2021
Published: November 11, 2021

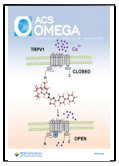

have discussed the evolution of coal particles during outburst.[11−13] However, there is no definite coal crushing index.

In this study, using the self-developed gas release experimental equipment, the effects of different gas pressures and gas adsorption properties on the ejection and crushing of coal particles during the rapid gas release process were simulated. Also, the fractal dimension method is used to compare and analyze the pulverized coal with different particle sizes. Based on the theory of crushing work and energy, we proposed a crushing index to express the crushing of coal particles.

2. TENSILE FAILURE MECHANISM OF COAL PARTICLES

During the formation of the coal body, it has experienced a variety of complex tectonic movements, which prompt the coal body to randomly distribute different structural planes, cracks, and other defects. When the internal cracks propagate, it will cause the instability failure of the coal and rock masses. Through many uniaxial compression tests, it can be confirmed that the occurrence and expansion of cracks are caused by tensile stress. The development process of the crack will make the primitive fissures of the coal body no longer bear the tensile stress, so that the tensile stress area will shift outward and expand. The pore gas pressure in the coal body will also cause the coal body to withstand stretching. It will promote the generation and development of cracks.

When there is gas in coal, the free gas acts on the wall of fractures and pores, which will cause tension on the coal body. Put coal particles into a closed cavity and fill the gas with a specific pressure. When the pore gas pressure P_i is the same as the gas pressure P_0 of the pressure-bearing cavity, the gas is in a dynamic equilibrium state. The gas diffusion and seepage inside the coal particles are much lower than the pressure relief speed of the pressure-bearing cavity when the gas in the pressure-bearing cavity is suddenly and quickly released. Therefore, the pressure difference between the interior and the exterior of the coal particles will quickly form $\Delta P(\Delta P = P_i - P_0)$, as shown in Figure 1. The crack propagation and coalescence under the tension of the free gas result in macroscopic rupture when the pressure difference increases rapidly and exceeds the strength of the coal body.

To achieve the effect of crushing, the following conditions need to be met in the experiment: (1) the gas pressure reaches the critical value of crack growth. The dynamic tensile failure of coal particles is the formation of tensile stress on the surface of the crack by gas. Therefore, the stress intensity factor at the crack tip will exceed the strength of the coal particles and cause the crack to propagate when the gas pressure is high enough. (2) Hermetic cavity can quickly relieve pressure. The formation of gas pressure difference depends on the gas release speed of the closed cavity. The gas pressure difference increased with an increase in the gas release speed.

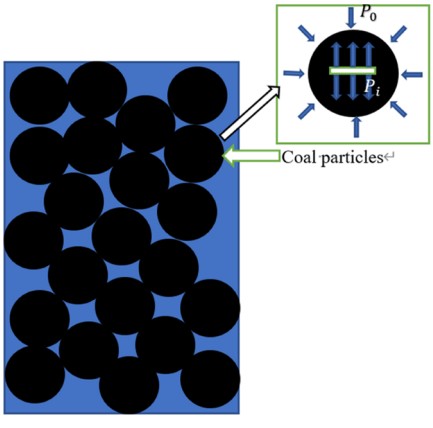

Figure 1. Forced state of coal particles in the hermetic cavity.

3. EXPERIMENTAL METHOD

3.1. Experimental Scheme. According to research,[14,15] different gas adsorption properties have different effects on coal particles in the process of high-pressure gas release. Therefore, two groups of experiments under the different gas stress conditions were designed to simulate the destruction of coal particles by different gas types. Because methane will be dangerous if it leaks during the experiment, this article chooses carbon dioxide, which has superior adsorption performance and higher safety than methane, to replace methane. In order to study the effect of adsorption performance on the experiment, we selected nitrogen, which has much lower adsorption than carbon dioxide, to compare the difference in adsorption. The first test group (Group I) was carried out using N_2. The second test group (Group II) was carried out using CO_2.The size of the coal particle diameter range was 3−10 mm. The total mass of coal particles is 1000 g, and the gas pressure settings are 0.6, 0.9, 1.2, 1.5, and 1.8 MPa, respectively, as shown in Tables 1 and 2. The schematic diagram of the experiment is shown in Figure 2. The coal sample selected for this experiment is the raw coal from the Donghuantuo Mine of Kailuan Group. The lump coal is collected from the working face of the coal mine, and it is packaged and transported to the laboratory. The experimental procedure of gas release included the following main steps (Figure 3). In the subsequent analysis of the results, in order to make the language concise, we abbreviate the mass of coal particles ejected in the experiment as ejected coal particle mass (ECM), and we abbreviate the total mass of coal particles as total coal mass (TCM).

Table 1. Experimental Scheme (Group I)

coal sample number	coal particle diameter/mm	coal particle quality/g	gas type	gas pressure/MPa
GY-1	3−10	1000	N_2	0.6
GY-2	3−10	1000	N_2	0.9
GY-3	3−10	1000	N_2	1.2
GY-4	3−10	1000	N_2	1.5
GY-5	3−10	1000	N_2	1.8

Table 2. Experimental Scheme (Group II)

coal sample number	coal particle diameter/mm	coal particle quality/g	gas type	gas pressure/MPa
GY-6	3−10	1000	CO_2	0.6
GY-7	3−10	1000	CO_2	0.9
GY-8	3−10	1000	CO_2	1.2
GY-9	3−10	1000	CO_2	1.5
GY-10	3−10	1000	CO_2	1.8

4. RESULTS AND DISCUSSION

4.1. Coal Particle Ejection Strength. The experimental results of the two experimental groups are shown in Tables 3

https://doi.org/10.1021/acsomega.1c05003
ACS Omega 2021, 6, 31253−31259

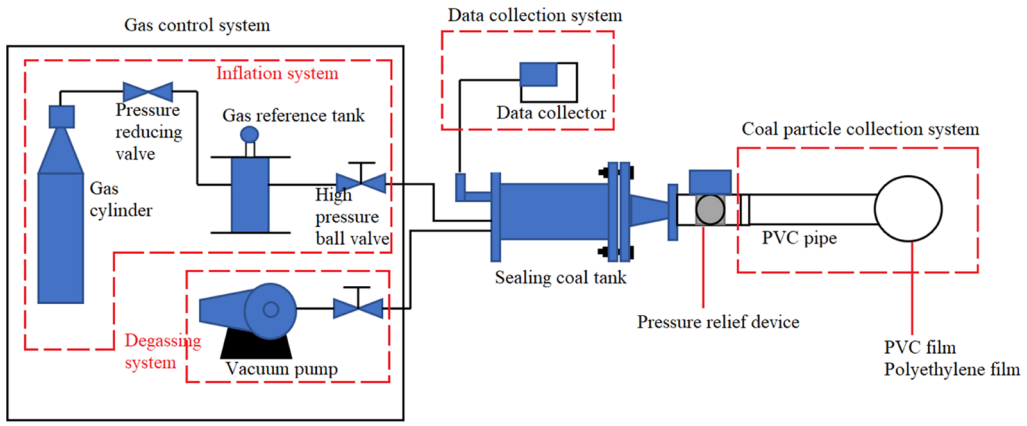

Figure 2. Schematic diagram of the experimental system.

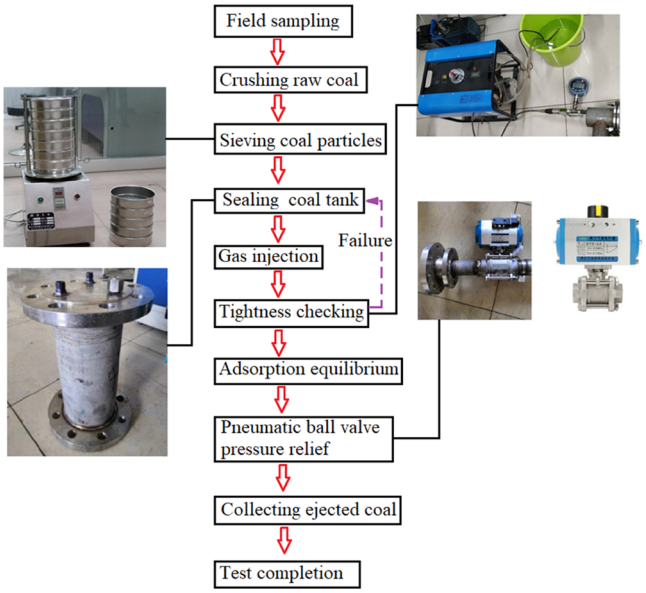

Figure 3. Flow chart of the high-pressure gas release experiment.

Table 3. Experimental Result of the Proportion of Coal Ejection Mass (Group I)

gas pressure/MPa	ECM/g	TCM/g	CES/%
0.6	81.9	1000	8.19
0.9	116.8	1000	11.68
1.2	101.6	1000	10.16
1.5	142.7	1000	14.27
1.8	190	1000	19

Table 4. Experimental Result of the Proportion of Coal Ejection Mass (Group II)

gas pressure/MPa	ECM/g	TCM/g	CES/%
0.6	100.7	1000	10.07
0.9	124	1000	12.4
1.2	175.4	1000	17.54
1.5	149	1000	14.9
1.8	217.1	1000	21.71

and 4 and Figure 4. To better analyze the experimental results, the coal particle ejection strength (CES) (i.e., the ratio of the ECM to the TCM) is proposed to express the influence of experimental factors on the destruction of coal particles. We

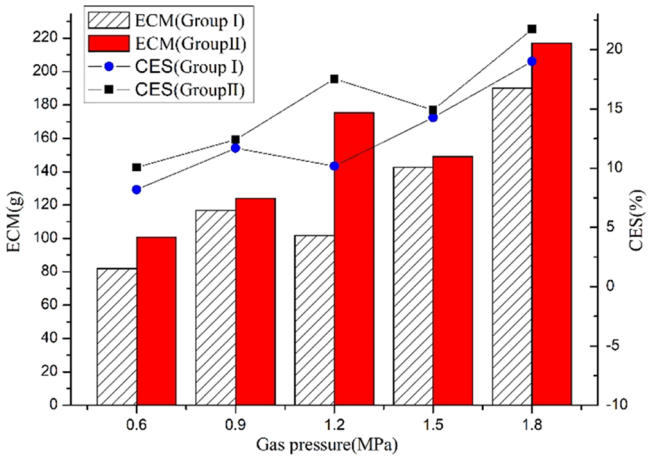

Figure 4. Experimental results of two test groups.

Table 5. Mass Ratio of Ejected Coal with Different Particle Sizes (Group I)

gas pressure/MPa	D_0 (%)	D_1 (%)	D_2 (%)	D_3 (%)	D_4 (%)	D_5 (%)	D_6 (%)
0.6	91.81	2.15	1.82	1.1	1.61	0.82	0.69
0.9	88.32	2.69	2.76	1.77	1.84	1.29	1.33
1.2	89.84	2.54	2.73	1.31	1.54	1.11	0.93
1.5	85.73	3.9	3.53	1.67	2.22	1.5	1.45
1.8	81	4.22	4.41	2.55	3.03	2.45	2.34

Table 6. Mass Ratio of Ejected Coal with Different Particle Sizes (Group II)

gas pressure/MPa	D_0 (%)	D_1 (%)	D_2 (%)	D_3 (%)	D_4 (%)	D_5 (%)	D_6 (%)
0.6	89.93	2.41	2.64	1.22	1.91	1.01	0.88
0.9	87.6	3.15	3.27	1.78	1.86	1.23	1.11
1.2	82.46	4.51	4.73	2.25	3.06	1.41	1.58
1.5	85.1	3.78	3.42	2.01	2.29	1.62	1.78
1.8	78.29	5.22	5.11	2.73	3.44	2.63	2.58

can see that with the increase of gas pressure, the coal ejection intensity of the two groups increased, indicating that gas pressure is an important factor affecting coal ejection. On the other hand, the different gas adsorbability also has a significant impact on the coal ejection strength. The value of CES increased with an increase of the gas adsorbability. However, the CES increased by 42.6% when the gas pressure increased

https://doi.org/10.1021/acsomega.1c05003
ACS Omega 2021, 6, 31253−31259

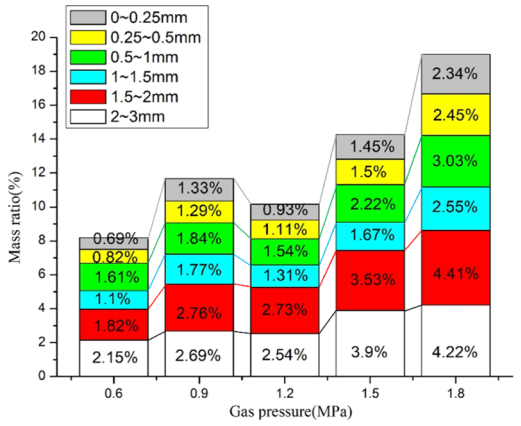

(a) Mass ratio of ejected coal with different particle sizes(Group I)

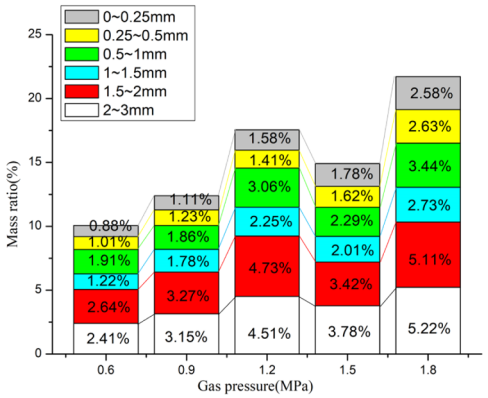

(b) Mass ratio of ejected coal with different particle sizes(Group II)

Figure 5. Mass ratio of ejected coal with different particle sizes.

Table 7. Fragmentation Index of Coal Particles (Group I)

gas pressure/MPa	0.6	0.9	1.2	1.5	1.8
W_g/J	15.5	27.31	39.95	53.17	66.82
h	3.30	5.83	8.53	11.35	14.27

Table 8. Fragmentation Index of Coal Particles (Group II)

gas pressure/MPa	0.6	0.9	1.2	1.5	1.8
W_g/J	6.6	11.7	17.1	22.8	28.6
h	1.42	2.50	3.66	4.8	6.12

from 0.6 to 0.9 MPa (Group I). Also, it increased by 40.44% when the gas pressure increased from 1.2 to 1.5 MPa (Group I). It increased by 33.14% when the gas pressure increased from 1.5 to 1.8 MPa (Group I). The change trend of Group II is similar to that of Group I. Therefore, the rising rate of CES gradually slows down as the gas pressure increases, and the relationship between CES and gas pressure is nonlinear.

4.2. Degree of Broken Coal Particles. The mass ratios of ejected coal with different particle sizes are shown in Tables 5 and 6 and Figure 5. To express the diameter range of coal particles conveniently, D_0, D_1, D_2, D_3, D_4, D_5, and D_6 are used to represent 3−10, 2−3, 1.5−2, 1−1.5, 0.5−1, 0.25−0.5, and 0−0.25 mm diameter ranges. The analysis of Group I shows that during the gas release, the mass ratio of ejected coal at stage D_1 increased from 2.15 to 4.22%, D_2 increased from 1.82 to 4.41%, and D_3 increased from 1.1 to 2.22%. D_4 increased from 1.61 to 3.03%, D_5 increased from 0.82 to 2.45%, and D_6 increased from 0.69 to 2.34%. The growth rates of ejected coal

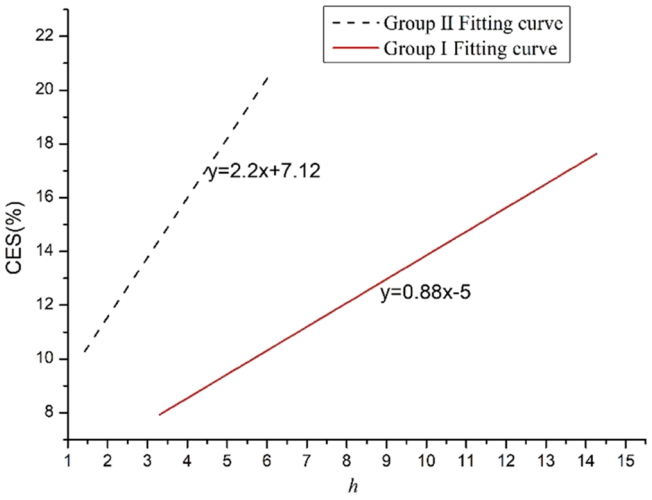

Figure 6. Fitting results of CES and fragmentation index h.

particle quality were 96.2, 142, 131.8, 88.1, 198, and 239%, respectively. Therefore, it can be seen that the gas release process has a certain tearing effect on the ejected coal particles, turning large-diameter coal particles into smaller-diameter coal particles. The greater the gas pressure, the greater the effect of coal particle being broken. The crushing effect of coal particles sprayed in Group II has a similar evolution, but Group II has stronger gas adsorption than Group I, and the mass ratio of coal particles sprayed in each stage is higher than Group I.

4.3. Coal Particle Fragmentation Index. In the process of high-pressure gas release, the gas pressure release time is between 0.15 and 0.26 s. We can regard the gas desorption time as a slow process compared with the gas pressure release time, so we do not consider the role of adsorbed gas in the gas release process. The following formula can express the energy in the process of coal particle crushing

$$W_{tr} + W_s = W_t + W_g \tag{1}$$

where W_{tr} is the transportation energy of coal particles and gas, W_s is the energy required for the crushing of coal particles, W_t is the elastic energy inside the coal particles, and W_g is the gas energy inside the coal particles.

According to a previous research,[16] the elastic energy inside coal particles is 2−3 orders of magnitude smaller than the energy inside gas. The energy inside the gas accounts for 98% of the total energy, so the elastic energy can be ignored in the process of coal crushing. Therefore, the energy of the coal particles' crushing process can be expressed by the following formula.

$$W_{tr} + W_s = W_g \tag{2}$$

The gas energy W_g can be expressed as

$$W_g = \frac{P_0 V_a}{\theta - 1}\left[\left(\frac{P_1}{P_0}\right)^{\theta - 1/\theta} - 1\right]\theta \tag{3}$$

where θ is the adiabatic index; P_1 is the gas pressure of coal particles, MPa; P_0 is the standard gas pressure, MPa; and V_a is the amount of free gas per unit volume of coal particles, m^3; V_a can be expressed as

$$V_a = \frac{\gamma P_1 T_0}{T_1 P_0 k} \tag{4}$$

https://doi.org/10.1021/acsomega.1c05003
ACS Omega 2021, 6, 31253−31259

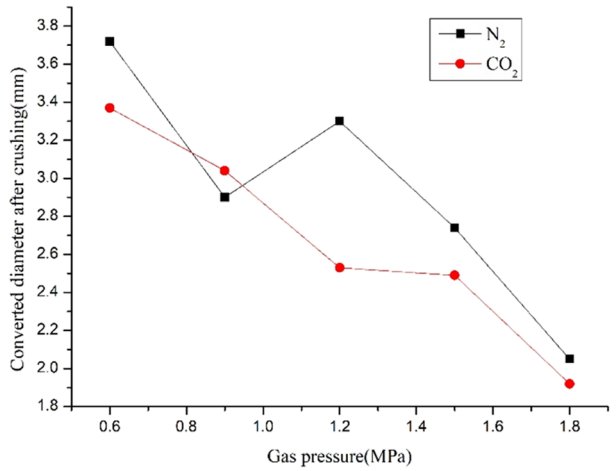

(a). Converted diameter after crushing

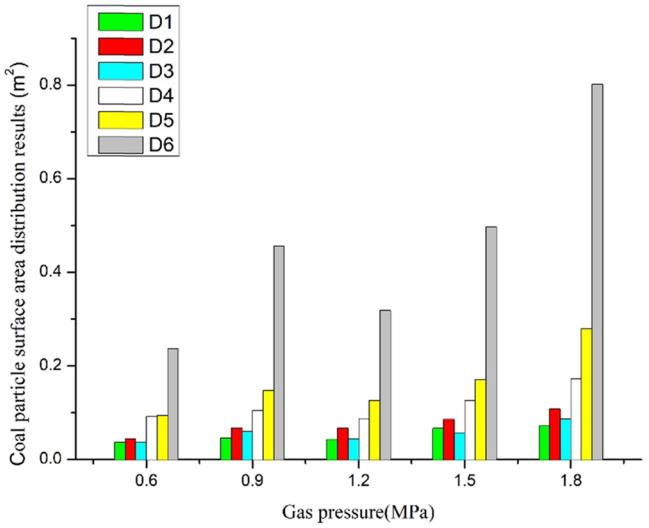

(b). Coal particle surface area distribution results(N_2)

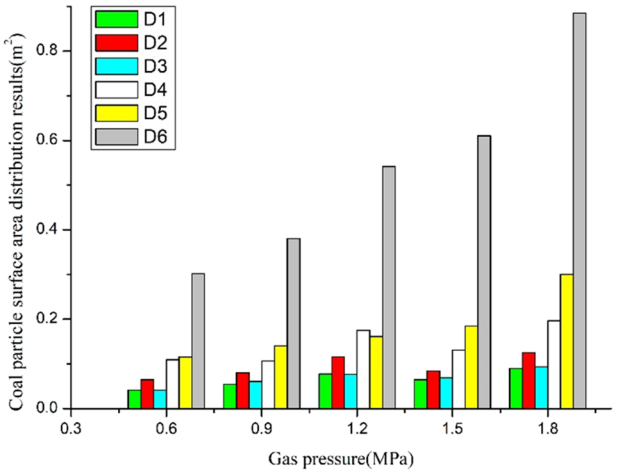

(c). Coal particle surface area distribution results(CO_2)

Figure 7. Coal particle-converted diameter after crushing and surface area distribution results.

where γ is the porosity per unit volume of coal; T_1 is the absolute temperature of coal seam gas; K; T_0 is the absolute temperature of the standard state, K; and k is the gas compression coefficient. According to the related theorem of thermodynamics, the relationship between temperature and pressure can be expressed as

$$T = \left(\frac{P}{nR}\right)^{\theta-1/\theta} \tag{5}$$

where n is the amount of substance, mol and R is the ideal gas constant, J/(mol·K). Combining formulas 3−5, the following formula can be obtained.

$$W_g = \frac{P_0\gamma}{k(\theta-1)}\left[\frac{P_1}{P_0} - \left(\frac{P_1}{P_0}\right)^{1/\theta}\right] \tag{6}$$

According to a previous research,[17] the crushing specific work W_p has a linear relationship with the firmness coefficient f. Therefore, the following formula can be obtained.[18−22]

$$W_s = W_p = 9.18f \tag{7}$$

Based on the new surface theory, the energy required for coal particle crushing is equal to the crushing specific work. The coal particle fragmentation index is proposed based on the above energy derivation formula.

$$h = \frac{W_g}{W_s} = \frac{\frac{P_0\gamma}{k(\theta-1)}\left[\frac{P_1}{P_0} - \left(\frac{P_1}{P_0}\right)^{1/\theta}\right]}{9.18f} \tag{8}$$

where h is the coal particle fragmentation index. The firmness coefficient f of the coal sample in this paper is 0.51.

The calculation results of W_g and h are shown in Table 7 and Table 8. The gas energy inside the coal particles increased with the gas pressure. The coal particle fragmentation index can indicate the difficulty of crushing coal particles during the process of gas release under the comprehensive influence of gas pressure and coal properties. The larger the fragmentation index, the higher the effect of coal particles being broken. The relationship between the CES and fragmentation index is shown in Figure 6. It can be seen from the figure that there is a good linear fitting result between CES and h, and their relationship can be expressed as

$$\mathrm{CES} = ah + b \tag{9}$$

where a is the slope of the fitting curve and b is the intercept of the fitting curve.

The slope of Group I is 0.88, which is smaller than the slope of Group II (2.2). The intercept of Group I is 5, which is also smaller than the intercept of Group II (7.12). The CES growth will be faster with the greater slope. Therefore, the slope of the fitting curve can show the intensity level of coal particle ejection. The larger the intercept, the easier it is for coal particles to break. Therefore, the intercept of the fitting curve can represent the critical point of coal particle ejection.

The firmness coefficient of coal is usually used to indicate the outburst state of the coal seam. The firmness coefficient is fixed during application. When the coal seam gas is extracted through preventive measures, there is no danger, although the f-value is still at a dangerous level. The coal particle fragmentation index in this study combines the firmness coefficient index, and the value of the fragmentation index can be updated according to the change in gas pressure. It can flexibly predict risk in the coal seam. It makes up for the

https://doi.org/10.1021/acsomega.1c05003
ACS Omega 2021, 6, 31253−31259

Table 9. Results of Linear Regression Analysis

gas type	$A = \frac{K}{d} + b$ (new surface theory)	$A = K \times \lg\frac{1}{d} + b$ (similarity theory)	$A = K \times \left(\frac{1}{\sqrt{d}}\right) + b$ (crack theory)
		R^2	
N_2	0.8975	0.8687	0.8850
CO_2	0.8910	0.9372	0.9158
average value	0.8943	0.9030	0.9004

shortcoming that the firmness coefficient does not consider the influence of gas pressure. The h index contains more information about coal particle breakage, which can reflect the crushing level of coal particles in the process of gas pressure release from two dimensions (a,b).

4.4. Rationality of Experimental Results. To determine the rationality of the experimental results, the average diameter of coal particles before crushing, the converted diameter after crushing, and the newly added surface area of coal particles are calculated by measuring the quality of coal particles in different diameter ranges before and after crushing (as shown in Figure 7). The coal sample's crushing energy and coal sample's converted diameter data were selected to perform linear regression analysis with three crushing theories (new surface theory, similarity theory, and crack theory). The analysis results are shown in Table 9. R^2 is the coefficient of determination of regression analysis, the average value of the new surface theory determination coefficient is 0.8943, the average value of the similarity theory determination coefficient is 0.9030, and the average value of the crack theory determination coefficient is 0.9004. It can prove that the crushing energy calculated by the experimental data and the newly added surface area conform to the crushing theory.

5. CONCLUSIONS

In this study, two groups of gas release experiments under different conditions were carried out using self-developed equipment to explore the crushing mechanism of coal particles in the gas release process. The main findings of this study are summarized as follows.

(1) By observing the entire experimental process of gas release, it was found that the gas release time is very short, and the free gas plays an important role in the entire pressure release process. In the process of gas release, the energy of free gas caused coal particles to be broken into small particles, and with the increase of gas adsorption and gas pressure, the crushing effect of coal particles increases. CES shows a nonlinear increase trend with the increase of gas pressure.

(2) The coal particle fragmentation index was derived based on the relationship between coal crushing energy and coal internal gas energy. Also, it is concluded that there is a linear relationship between CES and the fragmentation index h. The slope of the curve fitting can represent the intensity level of coal particle ejection, and the intercept of the fitting curve can represent the critical point of coal particle ejection. Fragmentation index can change dynamically with the change of certain conditions. The risk level of the coal seam can be flexibly predicted. It can provide a theoretical basis for the improvement of coal and gas outburst prevention methods.

(3) The self-developed equipment is a small-scale outburst of physical simulation equipment. With simple operation and short experiment time, the experimental data can be obtained quickly. The experimental data were obtained by fitting analysis with the three theories of the crushing energy theory which can show that the experimental data obtained by the experimental equipment are reasonable. However, this paper cannot measure the energy in the process of coal particle destruction. We will conduct numerical simulations or more precise tests in the follow-up work to monitor the energy changes during the destruction of coal particles.

DATA AVAILABILITY STATEMENT

All data, models, and code generated or used during the study appear in the submitted article.

AUTHOR INFORMATION

Corresponding Authors

Heng Zhang − *College of Emergency Management and Safety Engineering, China University of Mining and Technology (Beijing), Beijing 100083, P.R. China; China Academy of Safety Science and Technology, Beijing 100020, P.R. China;* orcid.org/0000-0003-4234-5165;
Email: zhanghengfawen@163.com

Min Hao − *College of Emergency Management and Safety Engineering, China University of Mining and Technology (Beijing), Beijing 100083, P.R. China;*
Email: haomin0926@163.com

Authors

Chengwu Li − *College of Emergency Management and Safety Engineering, China University of Mining and Technology (Beijing), Beijing 100083, P.R. China*

Xiaoqi Sun − *College of Emergency Management and Safety Engineering, China University of Mining and Technology (Beijing), Beijing 100083, P.R. China*

Complete contact information is available at: https://pubs.acs.org/10.1021/acsomega.1c05003

Notes

The authors declare no competing financial interest.

ACKNOWLEDGMENTS

This work was financially supported by the Research and Demonstration of Cloud Warning Technology for Gas Disasters Driven by Multidimensional Data (Qiankehe Support [2021] General 514).

REFERENCES

(1) Tutak, M.; Brodny, J.; Szurgacz, D.; Sobik, L.; Zhironkin, S. The Impact of the Ventilation System on the Methane Release Hazard and Spontaneous Combustion of Coal in the Area of Exploitation-A Case Study. *Energies* **2020**, *13*, 4891.

(2) Li, H.; Feng, Z.; Zhao, D.; Duan, D. Simulation Experiment and Acoustic Emission Study on Coal and Gas Outburst. *Rock Mech. Rock Eng.* **2017**, *50*, 2193−2205.

(3) Chen, L.; Wang, E.; Ou, J.; Fu, J. Coal and gas outburst hazards and factors of the No. B-1 Coalbed, Henan, China. *Geosci. J* **2018**, *22*, 171−182.

(4) Yuan, L. Control of coal and gas outbursts in Huainan mines in China: A review. *J. Rock Mech. Geotech. Eng.* **2016**, *8*, 559−567.

(5) Zhou, B.; Xu, J.; Yan, F.; Peng, S.; Gao, Y.; Li, Q.; Cheng, L. Effects of gas pressure on dynamic response of two-phase flow for coal-gas outburst. *Powder Technol.* **2021**, *377*, 55−69.

(6) Wang, C.; Yang, S.; Yang, D.; Li, X.; Jiang, C. Experimental analysis of the intensity and evolution of coal and gas outbursts. *Fuel* **2018**, *226*, 252−262.

(7) Dai, L.; Liu, Y.; Cao, J.; Yang, X.; Sun, H.; Wen, G.; Wang, B. A Study on the Energy Condition and Quantitative Analysis of the Occurrence of a Coal and Gas Outburst. *Shock Vib.* **2019**, *2019*, 8651353.

(8) Yin, G.; Jiang, C.; Wang, J. G.; Xu, J.; Zhang, D.; Huang, G. A New Experimental Apparatus for Coal and Gas Outburst Simulation. *Rock Mech. Rock Eng.* **2016**, *49*, 2005−2013.

(9) Black, D. J. Investigations into the identification and control of outburst risk in Australian underground coal mines. *Int. J. Min. Sci. Technol.* **2017**, *27*, 749−753.

(10) Ding, Y.; Yue, Z. Q. An experimental investigation of the roles of water content and gas decompression rate for outburst in coal briquettes. *Fuel* **2018**, *234*, 1221−1228.

(11) Guo, H.; Cheng, Y.; Ren, T.; Wang, L.; Yuan, L.; Jiang, H.; Liu, H. Pulverization characteristics of coal from a strong outburst-prone coal seam and their impact on gas desorption and diffusion properties. *J. Nat. Gas Sci. Eng.* **2016**, *33*, 867−878.

(12) Wu, X.; Peng, Y.; Xu, J.; Yan, Q.; Nie, W.; Zhang, T. Experimental study on evolution law for particle breakage during coal and gas outburst. *Int. J. Coal Sci. Technol.* **2020**, *7*, 97−106.

(13) Tu, Q.; Cheng, Y.; Ren, T.; Wang, Z.; Lin, J.; Lei, Y. Role of Tectonic Coal in Coal and Gas Outburst Behavior During Coal Mining. *Rock Mech. Rock Eng.* **2019**, *52*, 4619−4635.

(14) Sobczyk, J. A comparison of the influence of adsorbed gases on gas stresses leading to coal and gas outburst. *Fuel* **2014**, *115*, 288−294.

(15) Cao, J.; Dai, L.; Sun, H.; Wang, B.; Zhao, B.; Yang, X.; Zhao, X.; Guo, P. Experimental study of the impact of gas adsorption on coal and gas outburst dynamic effects. *Process Saf. Environ. Prot.* **2019**, *128*, 158−166.

(16) Wang, G.; Wu, M. M.; Cheng, W. M.; Chen, J. H.; Du, W. Z. Analysis of energy conditions for coal and gas outburst and factors influencing outburst intensity. *Rock Soil Mech.* **2015**, *36*, 2974−2982.

(17) Cai, C.; Xiong, Y. Theoretical and experimental study on crushing energy of outburst-proneness coal. *J. China Coal Soc.* **2005**, *30*, 63−66. CNKI:SUN:MTXB.0.2005-01-014

(18) Li, C.; Xu, Y.; Chen, P.; Li, H.; Lou, P. Dynamic Mechanical Properties and Fragment Fractal Characteristics of Fractured Coal-Rock-Like Combined Bodies in Split Hopkinson Pressure Bar Tests. *Nat. Resour. Res.* **2020**, *29*, 3179−3195.

(19) Wang, C.; Yang, S.; Li, J.; Li, X.; Jiang, C. Influence of coal moisture on initial gas desorption and gas-release energy characteristics. *Fuel* **2018**, *232*, 351−361.

(20) Chen, C.; Xu, J.; Okubo, S.; Peng, S. Damage evolution of tuff under cyclic tension-compression loading based on 3D digital image correlation. *Eng. Geol.* **2020**, *275*, 105736.

(21) Zhang, C.; Zhang, L. Permeability Characteristics of Broken Coal and Rock Under Cyclic Loading and Unloading. *Nat. Resour. Res.* **2019**, *28*, 1055−1069.

(22) Yin, G.; Li, M.; Wang, J. G.; Xu, J.; Li, W. Mechanical behavior and permeability evolution of gas infiltrated coals during protective layer mining. *Int. J. Rock Mech. Min. Sci.* **2015**, *80*, 292−301.

https://doi.org/10.1021/acsomega.1c05003
ACS Omega 2021, 6, 31253−31259